

## Supporting Information (SI)

### Four membered red iridium(III) complexes with Ir-S-P-S structures: rapidly room temperature synthesis and application in OLEDs

Ning Su, You-Xuan Zheng\*

<sup>1</sup> State Key Laboratory of Coordination Chemistry, Collaborative Innovation Center of Advanced Microstructures, Jiangsu Key Laboratory of Advanced Organic Materials, Nanjing National Laboratory of Microstructures, School of Chemistry and Chemical Engineering, Nanjing University, Nanjing 210093, P. R. China. E-mail: yxzheng@nju.edu.cn

<sup>2</sup> MaAnShan High-Tech Research Institute of Nanjing University, MaAnShan, 238200, P. R. China

†Electronic Supplementary Information (ESI) available. See DOI: 10.1039/x0xx00000x

#### Materials and Measurements.

All reagents and chemicals were purchased from commercial sources and used without further purification. <sup>1</sup>H NMR and <sup>19</sup>F NMR spectra were measured on a Bruker AM 400 spectrometer. High-resolution electrospray mass spectra (HRMS) was measured on G6500 from Agilent for complexes. TGA measurements were carried out on a DSC 823e analyzer (METTLER). Absorption and photoluminescence spectra were measured on a UV-3100 spectrophotometer and a Hitachi F-4600 photoluminescence spectrophotometer, respectively. The decay lifetimes were measured with an Edinburgh Instruments FLS 980 fluorescence spectrometer in degassed CH<sub>2</sub>Cl<sub>2</sub> solution at room temperature. The luminescence quantum efficiencies were calculated by comparison of the emission intensities (integrated areas) of a standard (*fac*-Ir(ppy)<sub>3</sub>) and the sample.

#### X-ray Crystallography.

The single crystals of complexes were carried out on a Bruker SMART CCD diffractometer using monochromated Mo K $\alpha$  radiation ( $\lambda = 0.71073 \text{ \AA}$ ) at 173 K. Cell parameters were retrieved using SMART software and refined using SAINT <sup>1</sup> on all observed reflections. Data were collected using a narrow-frame method with scan widths of 0.30° in  $\omega$  and an exposure time of 10 s/frame. The highly redundant data sets were reduced using SAINT and corrected for Lorentz and polarization effects. Absorption corrections were applied using SADABS <sup>2</sup>

supplied by Bruker. The structures were solved by direct methods with SHELXT-2014/5 and refined by full-matrix least-squares on  $F^2$  using the program SHELXL-2018/3.<sup>3</sup> The positions of metal atoms and their first coordination spheres were located from direct-methods E-maps; other non-hydrogen atoms were found in alternating difference Fourier syntheses and least-squares refinement cycles and, during the final cycles, refined anisotropically. Hydrogen atoms were placed in calculated position and refined as riding atoms with a uniform value of Uiso.

Details of cyclic voltammetry measurements and theoretical calculations.

Cyclic voltammetry measurements were conducted on a MPI-A multifunctional electrochemical and chemiluminescent system (Xi'an Remex Analytical Instrument Ltd. Co., China) at room temperature, with a polished Pt plate as the working electrode, platinum thread as the counter electrode and Ag-AgNO<sub>3</sub> (0.1 M) in CH<sub>2</sub>Cl<sub>2</sub> as the reference electrode, *tetra*-*n*-butylammonium perchlorate (0.1 M) was used as the supporting electrolyte, using Fc<sup>+</sup>/Fc as the internal standard, the scan rate was 0.1 V s<sup>-1</sup>. We perform theoretical calculations employing Gaussian09 software with B3LYP function.<sup>4</sup> The basis set of 6-31G(d, p) was used for C, H, N, O, F, P and S atoms while the LanL2DZ basis set was employed for Ir atoms.<sup>5</sup> The solvent effect of CH<sub>2</sub>Cl<sub>2</sub> was taken into consideration using conductor like polarizable continuum model (C-PCM).<sup>6</sup>

OLEDs fabrication and measurement.

All OLEDs were fabricated on the pre-patterned ITO-coated glass substrate with a sheet resistance of 15  $\Omega$  sq<sup>-1</sup>. The deposition rate for organic compounds is 1-2  $\text{\AA}$  s<sup>-1</sup>. The phosphor and the host 26DCzppy were co-evaporated to form emitting layer. The cathode consisting of LiF/ Al was deposited by evaporation of LiF with a deposition rate of 0.1  $\text{\AA}$  s<sup>-1</sup> and then by evaporation of Al metal with a rate of 3  $\text{\AA}$  s<sup>-1</sup>. The characteristic curves of the devices were measured with a computer which controlled KEITHLEY 2400 source meter with a calibrated silicon diode in air without device encapsulation. On the basis of the uncorrected PL and EL spectra, the Commission Internationale de l'Eclairage (CIE) coordinates were calculated using a test program of the Spectra scan PR650 spectrophotometer.

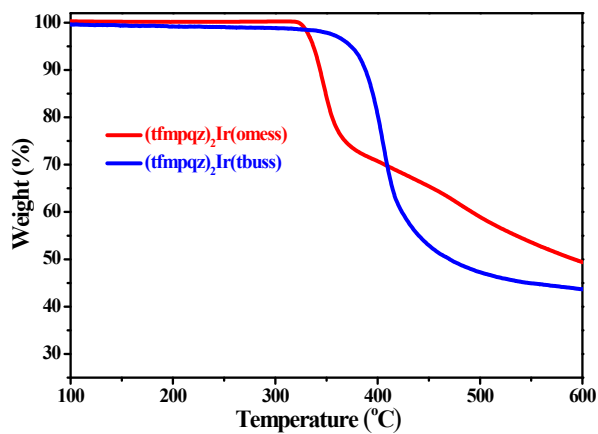


Fig. S1 TGA curves of  $(\text{tfmpqz})_2\text{Ir}(\text{omess})$  and  $(\text{tfmpqz})_2\text{Ir}(\text{tbuss})$  complexes.

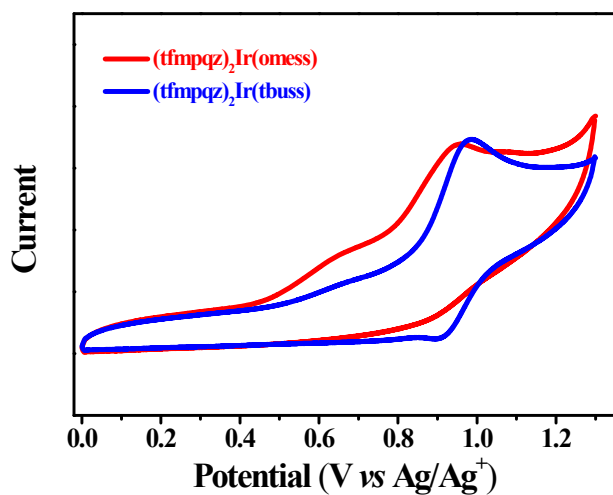


Fig. S2 CV curves of  $(\text{tfmpqz})_2\text{Ir}(\text{omess})$  and  $(\text{tfmpqz})_2\text{Ir}(\text{tbuss})$  complexes.

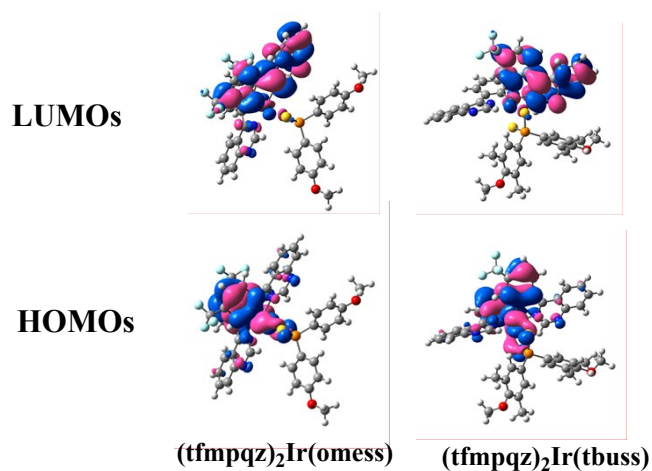


Fig.S3 Theoretical HOMO/LUMO electron distributions of two complexes.

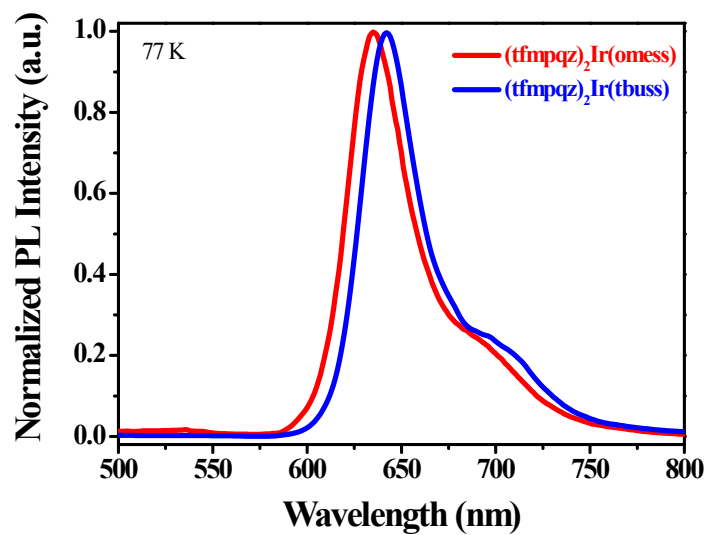


Fig.S4 the PL emissions of two complexes measured at 77 K.

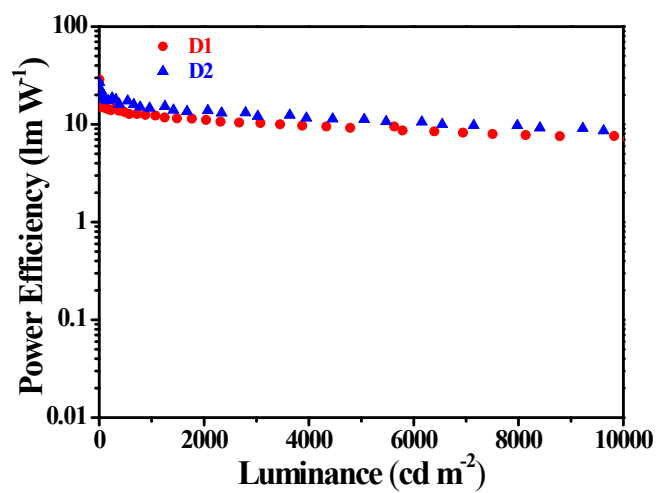


Fig.S5 Power efficiency ( $\eta_p$ ) versus luminance characteristics of two devices.

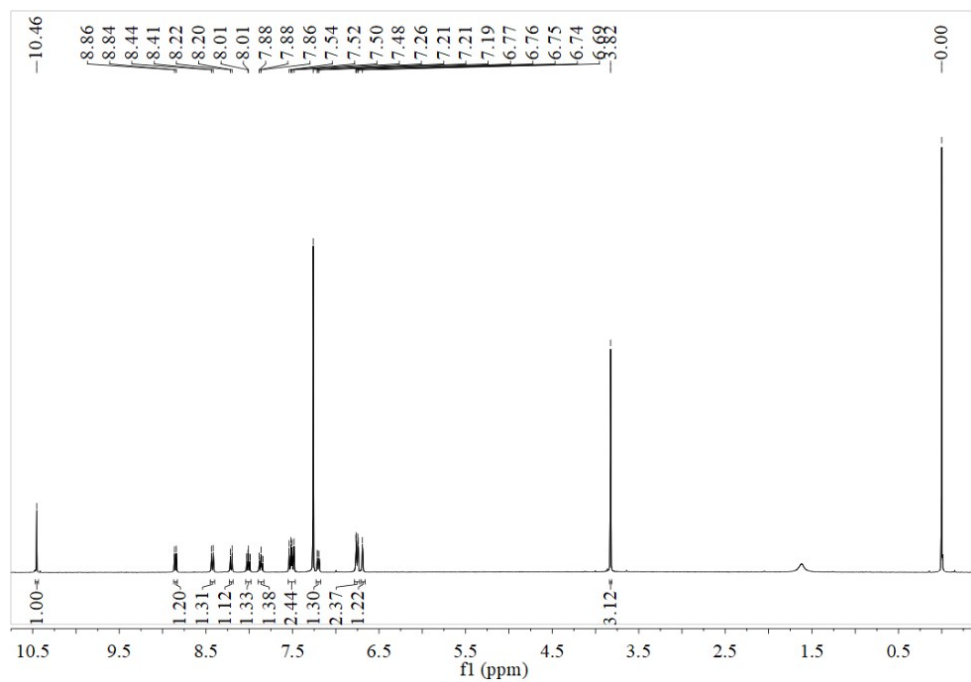


Fig. S6  $^1\text{H}$  NMR of  $(\text{tfmpqz})_2\text{Ir}(\text{omess})$  complex.

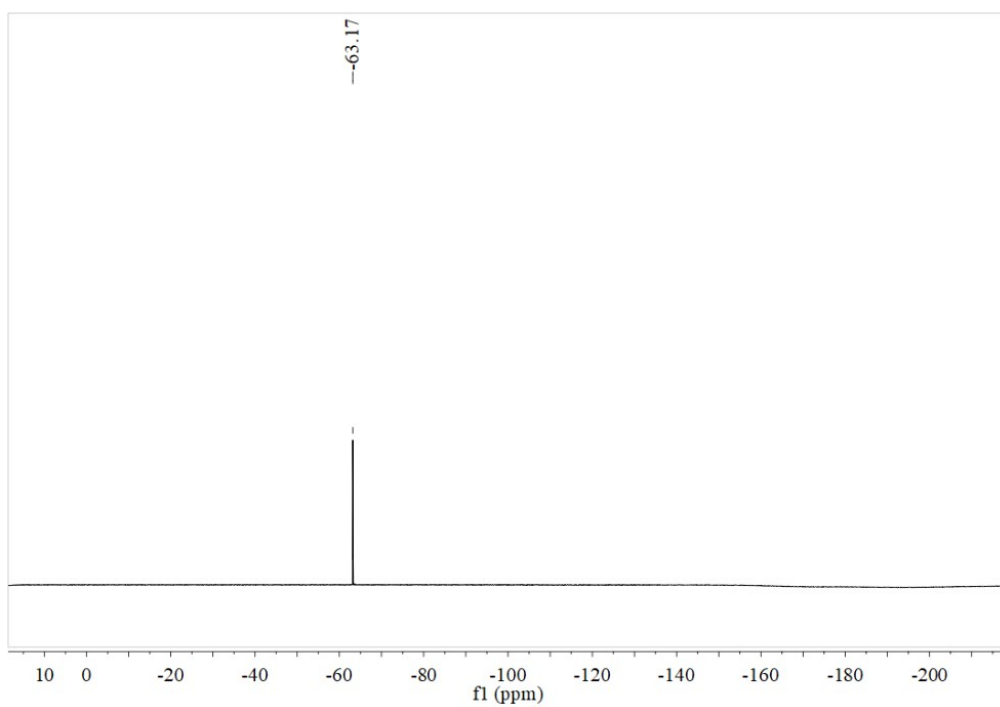


Fig. S7  $^{19}\text{F}$  NMR of  $(\text{tfmpqz})_2\text{Ir}(\text{omess})$  complex.

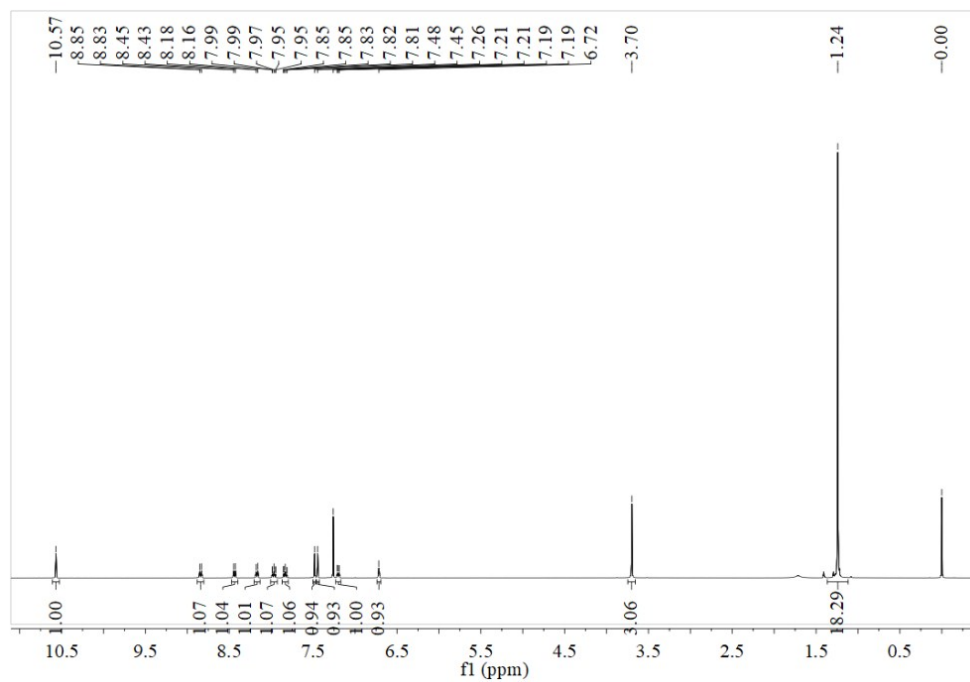


Fig. S8  $^1\text{H}$  NMR of  $(\text{tfmpqz})_2\text{Ir}(\text{tbuss})$  complex.

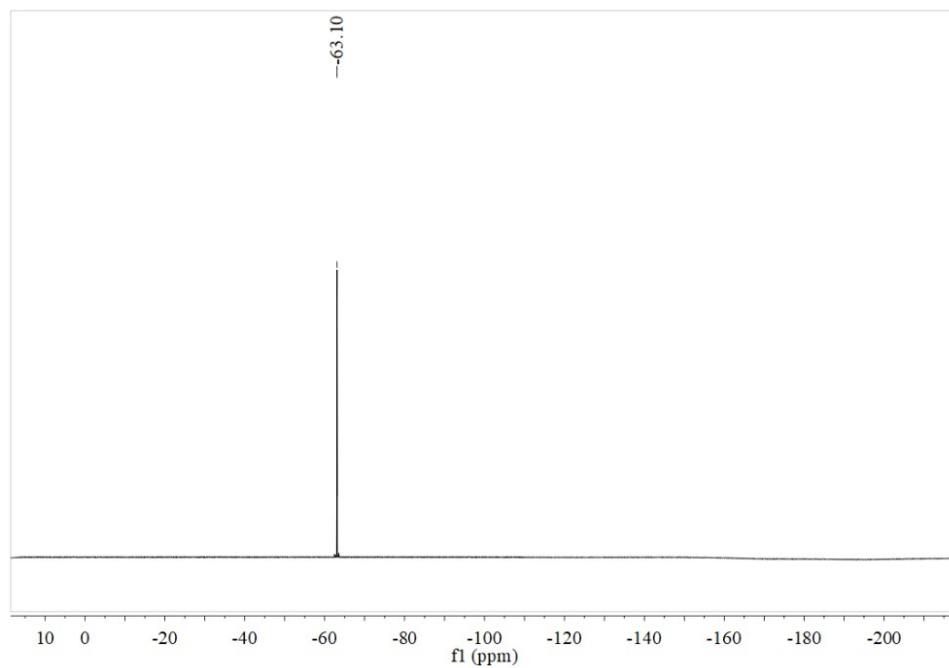


Fig. S9  $^{19}\text{F}$  NMR of  $(\text{tfmpqz})_2\text{Ir}(\text{tbuss})$  complex.

Table S1. Crystal information of (tfmpqz)<sub>2</sub>Ir(omess) complex.

(tfmpqz) <sub>2</sub> Ir(omess)	
Formula	C <sub>44</sub> H <sub>30</sub> F <sub>6</sub> IrN <sub>4</sub> O <sub>2</sub> PS <sub>2</sub>
Formula weight	1048.01
T (K)	173(2)
Wavelength (Å)	0.71073
Crystal system	Monoclinic
Space group	<i>P</i> 21/n
<i>a</i> (Å)	8.2405(7)
<i>b</i> (Å)	23.652(2)
<i>c</i> (Å)	20.2737 (18)
$\alpha$ (deg)	90
$\beta$ (deg)	93.404 (2)
$\gamma$ (deg)	90
<i>V</i> (Å <sup>3</sup> )	3944.4(6)
<i>Z</i>	4
$\rho_{\text{calcd}}$ (g/cm <sup>3</sup> )	1.765
$\mu$ (Mo K $\alpha$ ) (mm <sup>-1</sup> )	3.605
<i>F</i> (000)	2064
Range of transm factors (deg)	2.189-25.006
Reflns collected	23111
Unique( <i>R</i> <sub>int</sub> )	6944 (0.0474)
<i>R</i> <sub><i>I</i></sub> <sup><i>a</i></sup> , <i>wR</i> <sub>2</sub> <sup><i>b</i></sup> [ <i>I</i> > 2 <i>s</i> ( <i>I</i> )]	0.0436, 0.0918
<i>R</i> <sub><i>I</i></sub> <sup><i>a</i></sup> , <i>wR</i> <sub>2</sub> <sup><i>b</i></sup> (all data)	0.0771, 0.0971
GOF on <i>F</i> <sup>2</sup>	0.996
CCDC No.	1867812

$$R_1^a = \frac{\sum ||F_o| - |F_c||}{\sum F_o}, \quad wR_2^b = \left[ \frac{\sum w(F_o^2 - F_c^2)^2}{\sum w(F_o^2)} \right]^{1/2}$$

Table S2. Selected bond lengths of (tfmpqz)<sub>2</sub>Ir(omess) complex.

C6 - Ir1	2.002 (6)	P1 - S2	2.018 (2)	C21 - Ir1 - N3	78.6 (2)
C21 - Ir1	2.004 (6)	C35 - P1	1.811 (6)	C6 - Ir1 - N2	79.2 (2)
Ir1 - N3	2.038 (5)	C42 - P1	1.814 (7)	S2 - Ir1 - S1	79.37 (5)
Ir1 - N2	2.040 (5)	C31 - O1	1.426 (8)	S2 - P1 - S1	105.73 (10)
Ir1 - S2	2.5105 (16)	C32 - O1	1.368 (8)	C35 - P1 - C42	105.6 (3)
Ir1 - S1	2.5350 (16)	C38 - O2	1.413 (10)	C32 - O1 - C31	118.8 (6)
P1 - S1	2.024 (2)	C39 - O2	1.403 (9)	C39 - O2 - C38	117.9 (7)

Table S3. HOMO and LUMO electron cloud density distributions of each fragment of both Ir(III) complexes.

Complexes	Orbit	Composition(%)		
		tfmpqz	Ir atom	ancillary ligand
(tfmpqz) <sub>2</sub> Ir(omess)	HOMO	44.62	49.01	6.37
	LUMO	91.08	4.68	4.24
(tfmpqz) <sub>2</sub> Ir(tbuss)	HOMO	43.18	48.81	8.01
	LUMO	91.37	4.71	3.92

References:

1. *SAINTE-Plus*, version 6.02, Bruker Analytical X-ray System, Madison, WI, 1999.
2. Sheldrick, G. M. *SADABS An empirical absorption correction program*, Bruker Analytical X-ray Systems, Madison, WI, 1996.
3. Sheldrick, G. M. *SHELXTL-97*. Universität of Göttingen, Göttingen, Germany, 1997.
4. E. Runge and E. K. U. Gross, *Phys. Rev. Lett.*, 1984, 52, 997.
5. M. J. Frisch, G. W. Trucks, H. B. Schlegel, G. E. Scuseria, M. A. Robb, J. R. Cheeseman, G. Scalmani, V. Barone, B. Mennucci, G. A. Petersson, H. Nakatsuji, M. Caricato, X. Li, H. P. Hratchian, A. F. Izmaylov, J. Bloino, G. Zheng, J. L. Sonnenberg, M. Hada, M. Ehara, K. Toyota, R. Fukuda, J. Hasegawa, M. Ishida, T. Nakajima, Y. Honda, O. Kitao, H. Nakai, T. Vreven, J. A. Montgomery Jr., J. E. Peralta, F. Ogliaro, M. Bearpark, J. J. Heyd, E. Brothers, K. N. Kudin, V. N. Staroverov, R. Kobayashi, J. Normand, K. Raghavachari, A. Rendell, J. C. Burant, S. S. Iyengar, J. Tomasi, M. Cossi, N. Rega, J. M. Millam, M. Klene, J. E. Knox, J. B. Cross, V. Bakken, C. Adamo, J. Jaramillo, R. Gomperts, R. E. Stratmann, O. Yazyev, A. J. Austin, R. Cammi, C. Pomelli, J. W. Ochterski, R. L. Martin, K. Morokuma, V. G. Zakrzewski, G. A. Voth, P. Salvador, J. J. Dannenberg, S. Dapprich, A. D. Daniels, O. Farkas, J. B. Foresman, J. V. Ortiz, J. Cioslowski, D. J. Fox, *Gaussian 09, Revision A.01*, Gaussian, Inc., Wallingford, CT, 2009.
6. (a) P. J. Hay and W. R. Wadt, *J. Chem. Phys.*, 1985, 82, 299; (b) M. M. Francl, W. J. Pietro, W. J. Hehre, J. S. Binkley, M. S. Gordon, D. J. Defrees and J. A. Pople, *J. Chem. Phys.*, 1982, 77, 3654.